GAS RELATIVE PERMEABILITY AND FLOW BEHAVIOUR IN A RETROGRADE GAS/CONDENSATE RESERVOIR UNDER DEPLETION

by
O. Hjelmeland and L. Øyno, ResLab (Reservoir Laboratories AS), Trondheim, Norway,
S. R. Jakobssen, Petec, Stavanger, Norway
H. Niko, Shell Int. Petr. Maatschappij B.V., The Hague, The Netherlands

ABSTRACT

The dropout of retrograde liquid when depleting a gas/condensate reservoir below the dew point may lead to alterations of the gas flow behaviour. Near the wellbore, both gas and liquid condensate are expected to flow, resulting in a trapped gas saturation, whilst further out in the reservoir, the hydrocarbon liquid may be immobile until a critical condensate saturation is reached.

Because of its importance in field development, gas relative permeabilities at various hydrocarbon liquid saturations, together with critical condensate and trapped gas saturations, were determined for a North Sea gas/condensate field. Specially designed equipment was constructed for this purpose, and measurements were conducted under constant composition expansion on a long vertical composite core. Synthetic fluids and then real reservoir fluids at the appropriate conditions of pressure and temperature were used. To aid in the interpretation of the experiments, compositional simulations were also carried out.

For the case of the system with real reservoir fluids, the balance between gravitational and capillary forces was found to be of the greatest importance determining the distribution of the liquid condensate in the composite core.

The experiments, combined with numerical simulation, showed that, when the pressure has dropped sufficiently below the dew point, capillarity replaces gravity as the dominant force governing the distribution of liquid in the composite core. This explains the somewhat unusual shape of the measured gas relative permeability curve vs. liquid saturation. The force dependence on the flow behaviour is enhanced by the vertical flow in the heterogeneous core. The study also yielded realistic values of critical condensate and trapped gas saturations.

INTRODUCTION

Background

The depletion in retrograde gas condensate reservoirs will lead to a liquid phase condensation in the pores. Knowledge about the mobility and the onset of mobilization of this phase is of vital importance, both for production predictions and economic reasons. It is not only important to determine the mobility of the condensate phase, but also the mobility of the gas phase in distant areas and close to the well. In distant areas, the gaseous phase may still contain a large amount of heavy components. When the heavy components condense closer to the wellbore due to the lower pressure, the local condensate saturation may be large enough to be carried to the well and produced. Similarly, a high condensate saturation locally around the well may effectively decrease the productivity (of gas) to low levels.

Discussion of earlier work

Some work has been published on experiments designed to identify and solve the problems encountered in condensate wells. However, one of the main features in a depleting condensate reservoir is the low interfacial tension (IFT) between gas and fluid around the dew point, and a gradual increase in IFT in the reservoir both as a function of time (pressure) and as a function of distance towards the producing well. Early work was performed at ambient conditions, and some with fluids very different from reservoir fluids[1-4]. Kniazeft and Naville[1] used gas and water, and fixed the saturation by freezing the core. Gondouin et al[2] also used water instead of hydrocarbon condensate as the liquid phase, and the experiments were performed at ambient conditions. Ham et al[3] used a system of gasoline and nitrogen, but the experiments were still performed at ambient conditions. The low temperature and pressure experiments involve high IFT-values very far from the values actually found in the reservoirs. Many authors have found the trapping mechanism and relative permeability in a depleting gas condensate reservoir very dependent on IFT-values[4-7].

Since the interfacial tension is low in the vicinity of the dew point, gravity may dominate the flow behaviour and condensate saturation distribution. This has been extensively discussed by Williams and Dawe[8]. Water in the pores has been shown to have an effect, but the results are not conclusive. There are indications that the condensate wets the water (forms a wetting film) in the pores completely[9]. In a water-wet rock, the water will be stationary in the smallest pores and in irregularities in the pores. Thus the water may not play an important role. However, Saeidi and Handy[10] have shown that by using a methane-propane system at elevated pressures, the critical condensate saturation with water present is lower than without water in the pores. The wetting of the condensate as a function of the interfacial tension has been discussed by Ronde[11]. He explained the rela-

tive permeability behaviour close to the dew point as a result of wetting behaviour between the condensate and the pore walls. He claimed that the effect was due to the wetting undergoing a Cahn transition in the low IFT range. The possible influence of varying irreducible water saturation is not treated in this work.

The measurements of critical condensate saturation and gas relative permeability at reservoir conditions have been reported by a few authors. These experiments ensure IFT-values close to actual reservoir values, and wettability effects are also better simulated. Gravier et al[12] used a synthetic gas condensate system with IFT-values close to the reservoir values. They altered the temperature instead of the pressure to increase the condensate saturation in the core and simulate the depletion process. Eldon and Puckett[13] used recombined gas condensate and full reservoir conditions, but did not report gas relative permeabilities from their experiments. They did, however, perform experiments to quantify the critical condensate saturation and trapped gas saturation after condensate flooding.

Morel et al[14] performed an extensive study on the mobility of condensate in a depleting gas condensate field. They found a small mobility of condensate at pressures right from the dew point and lower, but stated that the mobility was very minute. The relative permeability curves had to be modified at low IFT-values. They did not measure the relative permeability to gas, but obtained these results only from simulation.

Purpose and Scope

According to the literature review, there is a need for experiments using real reservoir rocks and fluids where gas relative permeability and critical condensate saturation is studied in a depleting gas condensate reservoir. It is expected that the figures measured for one particular reservoir may differ from the next because of differences in pore network, capillary pressure, water saturation and wettability.

The primary goal of this study has been to develop a methodology to measure gas relative permeability and critical condensate saturation under realistic conditions.

EXPERIMENTAL

Experimental design

A special equipment was custom-designed for the purpose of studying gas condensate flow and depletion.
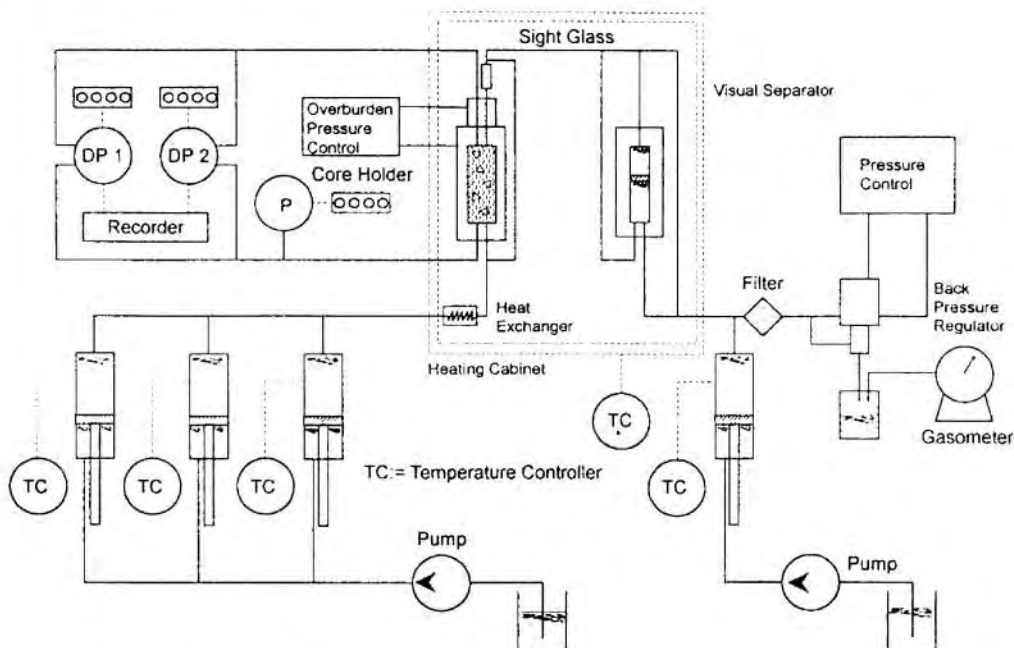
Figure 1: *Flow diagram for gas condensate studies*

A schematic flow diagram of the equipment is shown in Figure 1. The equipment is constructed for 69 MPa (10,000 psi) and 180°C (350°F) flow conditions. The core holder is vertically positioned in an oven, and can take a composite 1½ inch diameter core of up to 60 cm length. Independent axial and radial load up to 103 MPa (15,000 psi) may be applied. A high pressure displacement pump may give constant pressure or constant rate displacements or may be programmed for depletion at a given rate. Fluids are transferred from heated piston bottles into the core, passing through a heat exchanger to ensure the right temperature of the fluids.

A pressure control unit regulates all "overburden" pressures and monitors differential pressures. At top of the core (outlet) a visual sight glass is positioned and a video-camera records changes in production schemes (gas, fluids or mixtures). Produced fluids from the cores enters into a visual high pressure separator and are collected there for measurements. Excess fluids are either produced through a back pressure system into atmospheric conditions, or are produced into a piston vessel under controlled retracting pumping mode.

The core material was from a North Sea gas condensate reservoir. Four seal peels from a "clean" sandstone layer were selected based on permeability estimates from logs. The plugs of 1.5" diameter were drilled horizontally from the seal peels, The plugs were carefully prepared; trimming, cleaning, drying and then porosity and permeability were determined on each.

Core material

One composite core was assembled giving a total length of 50 cm. With a limited number of core samples, it was tried to make up as homogeneous composite core as possible. The individual permeabilities ranged from 70 mD to 340 mD in the composite core. Individual plug porosities ranged from 17 to 26 percent.

Fluids

The brine was made as a synthetic brine based on water analysis from the reservoir.

Two gas condensates were used; first a synthetic gas condensate, later live reservoir gas condensate. The synthetic gas condensate was made to be identical to the fluid used by Gravier et al[12] (75.95 percent methane, 20.89 percent n-pentane and 3.16 percent n-nonane).

Figure 2: *Measured liquid dropout curve compared to literature values*

All measurements using the synthetic condensate were performed at 16.0 MPa and the temperature was altered instead of the pressure as should be done in a real gas condensate system under depletion. The dew point at 16.0 MPa for the fluid was measured to 132.9°C, and the maximum liquid dropout was 51 % liquid at 30°C. The liquid dropout curve can be seen in Figure 2. From a temperature of 90°C and down, there is a good correspondence between our measurements and those by Gravier et al[12].

The real gas condensate system was recombined from separator gas and oil samples. The composition and relevant data are found in Table 1. The liquid dropout curve was derived from a constant composition experiment and using pressure steps of 1.0 MPa starting above dew point pressure.

Table 1: *Properties of the real gas condensate system*

Component	Mol %	
N_2	0.22	
CO_2	3.60	
C_1	73.79	
C_2	7.50	
C_3	4.21	
iC_4/nC_4	2.01	
iC_5/nC_5	0.94	
C_6	0.55	
C_7+	7.18	
Molecular weight of C_7+ (calculated)	190	
Reservoir temperature	130°C	
Dew point pressure	45.6 MPa	

Synthetic gas condensate experiments

The "depletion" in the reservoir was simulated by a reduction in temperature in the core, the assumption being that the liquid drop out in the pore space similar to the process of pressure reduction. Using this method of temperature reduction, it is possible to obtain a large retrograde condensation in the core. A diagram of the experimental scheme is shown in Figure 3.

During "depletion", measurements of effective permeabilities were performed, and at the last step, critical gas saturation was determined.

Recombined reservoir gas condensate experiments

Depletion in the long core was carried out similarly to the process in the reservoir. The core and the initial procedures were identical to the previous phase. Initial conditions when the core contained gas-condensate above dew point pressure were; pore pressure 50 MPa, temperature 130°C and net overburden pressure 19 MPa (hydrostatic). The experimental flow scheme is shown in Figure 4.

The gas relative permeability was measured by reducing the pore pressure in steps, maintaining a constant rate of depletion during each step of 15 kPa/min. Reaching the desired pressure level, an equilibrium time of at least 20 hours was used to allow the gas and liquid to reach equilibrium in the core and connected bottle. After the equilibrium period, equilibrium gas from the connected gas and condensate bottle was flooded into the bottom of the core to determine the gas permeability. The gas permeability measurements were performed at several low rates at each pressure- (and thus saturation-) step close to the dew point. The rates were comparable to reservoir rates. At pressure steps of 35.5 MPa and below, significantly higher gas flooding rates were used after the initial low rate measurements had been performed. Low rate measurements were then again performed, before pressure depletion was initiated to reach the next pressure step.

At the pressure corresponding to maximum liquid dropout (25.0 MPa), a flood using equilibrium condensate (liquid phase in equilibrium with gas at 25.0 MPa) was performed
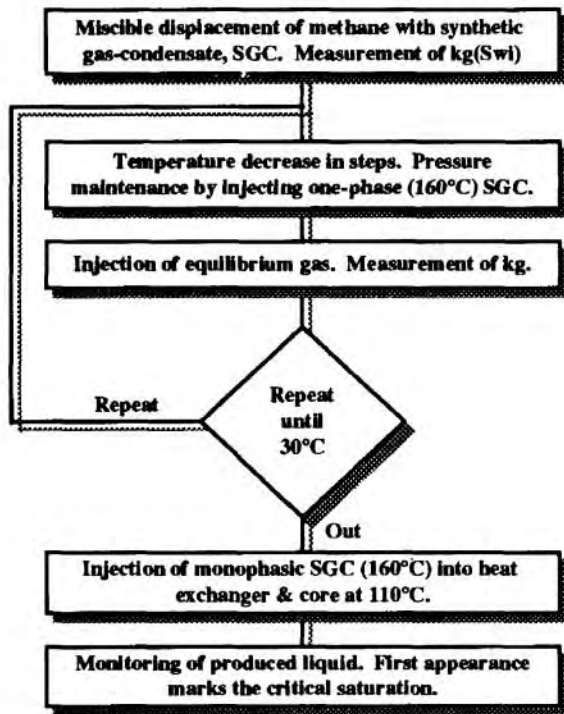
Figure 3: *Experimental flow diagram of synthetic gas condensate (SGC) experiments*
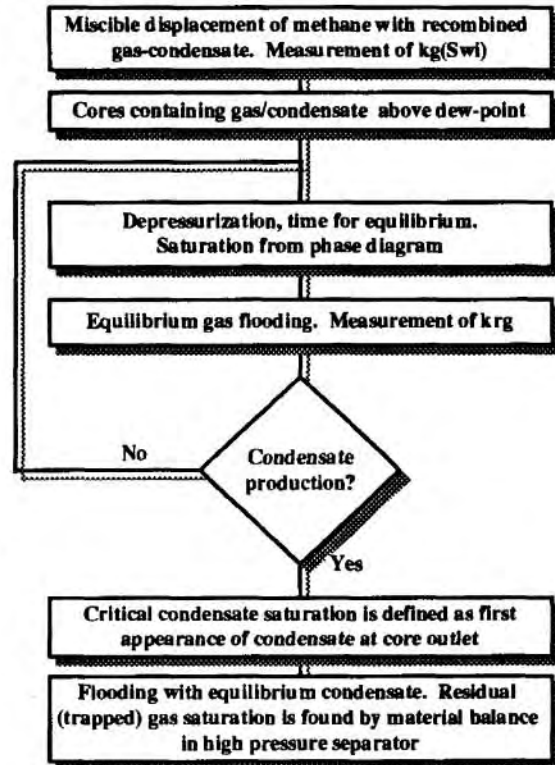
Figure 4: *Experimental flow diagram of experiments with real gas condensate*

into the bottom of the vertical core. Condensate flooding was performed until no more gas was produced from the core and the differential pressure across the core was constant. At this point, calculation of trapped gas saturation was possible. The injection rate of condensate was comparable to reservoir rates.

After finishing the experiments, the complete experimental sequence was reproduced on the same core in order to confirm experimental trends.

Numerical simulation

In order to verify the experimental results, a simulator able to model the relative permeability as a function of IFT was employed. The FRAGOR compositional simulator with the Peng-Robinson equation of state was used for the purpose.

In the model, the shape of the gas and condensate relative permeability is given by the empirical correlations;

$$kro = kro_0 \, (So*)^{\frac{2+3\lambda}{\lambda}} \quad and \quad krg = krg_0 \, (1-So*)^2 (1-So*)^{\left(\frac{2+\lambda}{\lambda}\right)}$$

where kro_0 and krg_0 are the end point relative permeabilities of condensate and gas, respectively. $So*$ is the normalized oil saturation, and λ is the average pore size distribution coefficient. The capillary pressure is in FRAGOR modelled as a function of interfacial tension;

$$Pc(\sigma) = Pc_0 \left(\frac{\sigma}{\sigma_0} \right)$$

Pc_0 is the capillary pressure at the interfacial tension σ_0. $Pc(\sigma)$ is the capillary pressure at the interfacial tension σ.

The change in residual/critical saturation and the relative permeability with interfacial tension is modelled by FRAGOR as;

$$Soc = f(\sigma)Soc_0 \quad where \quad f(\sigma) = \left(\frac{\sigma}{\sigma_0} \right)^{1/n}$$

$$kro(\sigma) = f(\sigma)kro(\sigma_0) + (1-f(\sigma))\frac{So}{1-Sw}$$

$$krg(\sigma) = f(\sigma)krg(\sigma_0) + (1-f(\sigma))\frac{Sg}{1-Sw}$$

Soc_0 is the critical condensate saturation at interfacial tension σ_0, and n is a correlation factor.

The input critical saturation to the simulation model is defined at high interfacial tension (low pressure), and the model then calculates changes in critical condensate saturation as a function of pressure (interfacial tension). The Capillary and the Bond number for the experiment will change with pressure since both interfacial tension, viscosity and density changes. In addition, the capillary number also changes with rate.

Input to the simulations were the measured composition and properties of the gas condensate and measured capillary pressures. The phase package is based on Peng-Robinson EOS using nine pseudo components. Viscosities were calculated from the pVT-package, pVTx, using the Lohrenz, Bray and Clark-correlation. The model calculates the capillary pressure and the relative permeability both as a function of saturation and as a function of interfacial tension. Each of the seven individual cores plugs were modelled by three numerical blocks and, in addition, two well blocks were used, one for the producer and one for the injector. The laboratory procedures are reproduced with respect to core pressures, injection rates and flood time periods.

The first phase of the simulation assumed ambient input relative permeability curves based on the Corey equations[15] using capillary pressure curves to obtain the Corey expo-

nent. The simulation gave calculated relative permeabilities over the core and condensate saturation distribution at different pressure steps.

The second phase of the numerical simulation study was aimed at accepting the experimentally determined gas relative permeabilities, and calculating the input relative permeabilities necessary to match the experiments. This implies a curve different from the Corey type used in the first phase. Through trial and errors, the input gas relative permeability was adjusted so that the calculated effective gas permeability was closer to the experimental data.

RESULTS AND DISCUSSION

Initial conditions

Table 2 gives a summary of the initial conditions of single cores and the composite core. Between the experiments, the composite core was cleaned and a new water saturation was established.

Table 2: *Petrophysical properties of the material used in the experiments and initial conditions of composite core*

		Phase I	Phase II
Single cores		*Range*	*Range*
Water permeability, k_w	(mD)	64-297	64-297
Helium porosity, φ_{He}	(%)	16-25	16-25
Composite core			
Water permeability, k_w	(mD)	76.4	90.0
Gas permeability at irreducible water saturation	(mD)	59.3	61.3
Initial water saturation (Phase II), S_{wi}	(% PV)	20.6	15.8

Experimental results

Figure 5 shows the gas relative permeability curve obtained on the synthetic gas condensate, plotted versus condensate saturation. The critical condensate saturation was found to be 29 percent (of PV) with a gas relative permeability of 0.30 at this point.

In the experiments using real gas condensate, two identical experiments were performed with the same core as in the first experiment. These experiments did not give a smooth gas relative permeability as was found with the synthetic gas condensate system. (Figure 5) At a condensate saturation of about 10-12 percent the curves started to increase despite an increasing condensate saturation. Several relative permeability measurements at different flow rates were performed, and all verified
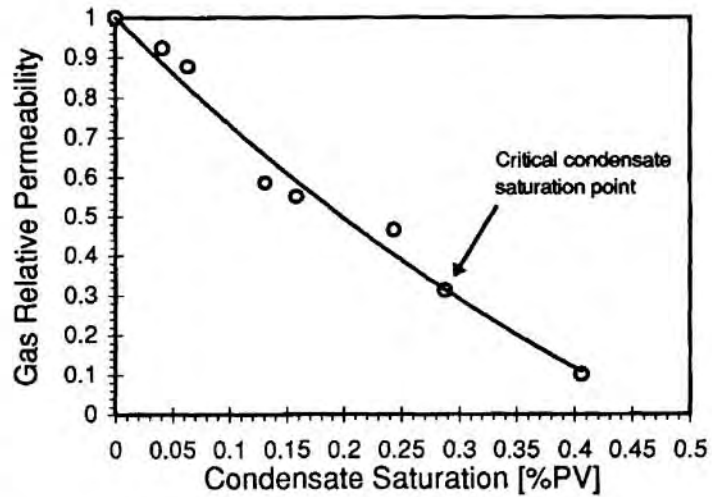
Figure 5: *Gas relative permeability curve measured using synthetic gas condensate*

this phenomenon; there was a local maximum in relative permeability at about 16 - 20 percent condensate saturation and then a further decrease with increasing saturation. The condensate saturation in the core was found from Pvt.-measurements, assuming that the saturation did not change during flooding.

The maximum obtainable condensate saturation was 19.7 % PV (corresponding to 24 % HCPV) and therefore no critical condensate saturation was determined. (Expected to be closer to 30 % PV.) No condensate production was monitored, but in the simulation study a minor production was found. However, the volumes were too small to be measured during the experiments. The trapped gas saturation after injecting equilibrium condensate was found to be 24.9 % PV. All gas and condensate saturation values were calculated from PVT studies, and complete equilibrium between gas and condensate was assumed.

Interpretation of experimental results by numerical simulation

In the first part of the simulation study, experimental results from the real gas condensate system were tried to be matched using Corey type relative permeabilities, however, without success. Results were compared at different critical condensate saturations. The second part allowed modifications to the input relative permeability curves to match the experimental results.

Due to the difference in petrophysical characteristics for the single core plugs, the simulation study found that the critical condensate saturation was non-uniform in the com-

Due to the difference in petrophysical characteristics for the single core plugs, the simulation study found that the critical condensate saturation was non-uniform in the composite core. As pressure decreased, the difference in saturation between single cores increased. The condensate saturation distribution for the composite core for different scenarios are found in Figure 6. It can be seen that at 44 MPa, the saturation distribution is uniform throughout the system while at 29 MPa there is a great span in saturations. This non-uniformity is dependent on the assumed critical condensate saturation and is caused by the inhomogeneity of the system. This large span of condensate saturations is caused by a balance of the fluid density gradient and the capillary force between the single core plugs in the composite core.
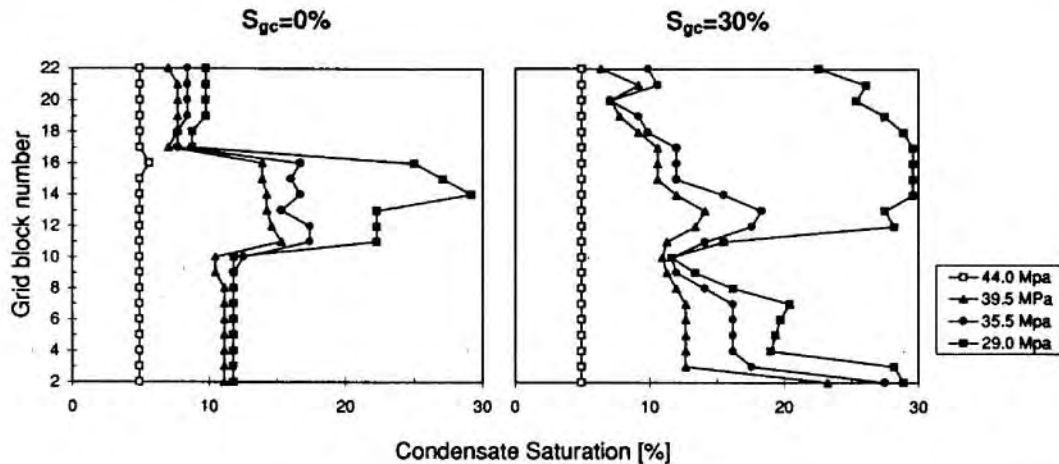
Figure 6: *Numerically simulated condensate saturation distribution in the composite core at different pressures and with critical condensate saturations of zero and 30 percent, respectively*

The calculated gas relative permeability curves from the numerical simulation study is shown in Figure 7 and compared to the experimental values. The first set of curves are generated based on ambient relative permeability curves from the Corey equations. The second set shows the gas relative permeabilities, aimed at matching the experimental gas relative permeability curves. It is evident that, in this non-uniform system, there is not a "smooth" gas-relative permeability relationship.

In the early stage of the depletion, the saturation distribution is almost exclusively gravity controlled. In this case the relative permeability to gas decreases as expected when increasing the condensate saturation. When the flow mechanisms are dominated by capillary pressure in the medium pressure range, the condensate saturation is fairly high at the ends, caused by end effects. The condensate saturation in the middle core is also high, probably caused by imbibition into the core underneath and redistribution of the fluid into this core plug by viscous forces. This process is thus flow rate dependent, and may be the
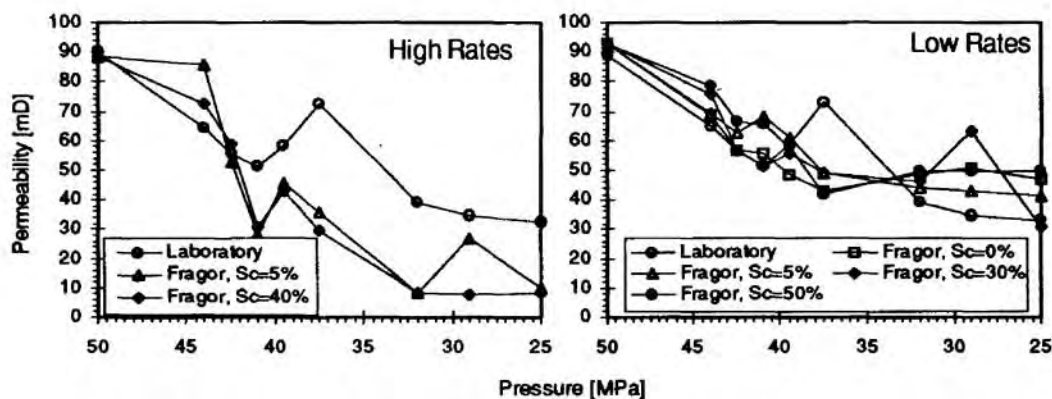
Figure 7: *Effective permeabilities to gas as a function of pressure (saturations) for different critical gas saturations*

Left: Simulation assuming Corey-type relative permeabilities
Right: Matching of simulated and experimental relative permeability curves

reason for the relative permeability dependence on flow rate, observed both in the numerical simulation and experiments.

The key to understanding the derived average relative permeabilities for the entire length of the composite core lies in the prevailing condensate saturations calculated for the individual core pieces. Figure 6 shows condensate saturation profiles over the entire core length at various pressure levels and for 2 assumed values of the (initial) critical condensate saturation, namely 0 and 30 %. Let us assume for the moment that 30% is the more likely case based on the matches shown in Figure 7. We could then derive from the simulation, that, as long as flow is mainly gravity dominated, condensate saturations increase over most of the core length, resulting in a continuous decrease of the averaged gas relative permeability. When capillary pressures start to dominate flow (lower pressure, higher IFT, i.e. at 29.5 MPa and 35.5 MPa in Figure 6.), we see accumulation of relatively high condensate saturations at the bottom and in the middle of the composite core which happen to be core pieces of relatively high permeability. This may explain the temporary increase in the average gas relperms at this stage, see figure 7. It should also be obvious that these averaged gas relperms are rate sensitive, as viscous forces have also a considerable influence on the redistribution of condensate saturations over the composite core. Although this was not tried it is worth noting that a relative permeability model in which relperms are both IFT and velocity dependent might have explained the experimental results even better.

The reason why the relative permeability curve of the synthetic gas condensate does not show the same behaviour may be a combination of two effects. The IFT-values, which partly determine the capillary forces in the sample, are lower in the middle saturation

12

range for the synthetic gas condensate. This delays or eliminates the effect of capillarity on the relative permeability pressure curve. The fluid phase in the real condensate is heavier than the fluid phase in the synthetic system, rendering the influence of gravity forces in the real system more important. This difference may also explain the difference in gas relative permeability curve shape between the two systems.

CONCLUSIONS

1. The numerical simulation was able to match the gas relative permeability *shape* by using a Corey type input relative permeability curve based on capillary pressures. By modifying the input (ambient condition) gas/oil relative permeability curves, a better match between the experimental and simulated curves could be found. The simulation clearly showed the transition between purely gravity controlled saturation distribution to a distribution controlled both by gravity, capillary and viscous effects. Gravity dominates close to the dew point. Saturation distribution in the reservoir will be strongly affected by this interaction, and must be taken into consideration when simulating the production. These forces may play an important role also at reservoir field scale.

2. The critical gas saturation found on the synthetic gas condensate of 29 % fits previously reported data. The relative permeability curve measured in the synthetic gas condensate gave a smooth and "normal" trend.

3. The trapped gas saturation after equilibrium condensate flooding was measured and found to be 24.9 % PV for the studied reservoir, using real reservoir gas condensate.

   Numerical simulation was able to match the experimental results when the dependence of IFT was taken into account on the relative permeability curves. The simulation clearly demonstrated the condensate saturation distribution variation at different pressures, and was useful for understanding the different mechanisms.

ACKNOWLEDGMENT

NOMENCLATURE

P_c	=	capillary pressure
PV	=	Pore volume (cm^3)
HCPV	=	Hydrocarbon pore volume (cm^3) = PV (1 - S_{wi})
S_{wi}	=	Initial water saturation (% or fraction)
S_{gr}	=	Residual gas saturation (% or fraction) after condensate flood
S_c	=	Condensate saturation (% or fraction)
S_g	=	Gas saturation (% or fraction)
S_0	=	oil (condensate) saturation
φ_{He}	=	Helium porosity (% or fraction)
k_w	=	Water permeability at 100 % water saturation (k_{abs}) (mD)
$k_o(S_{wi})$	=	Oil permeability at initial water saturation (mD)
$k_g(S_{wi})$	=	Gas permeability at initial water saturation (mD)
k_{rg}	=	Gas relative permeability
k_{ro}	=	oil (condensate) relative permeability
λ	=	average pore size distribution coefficient
σ	=	interfacial tension (mN/m)

REFERENCES

/1/ Kniazeff, V.J. and Naville, S.A.: "Two Phase Flow of Volatile Hydrocarbons", Soc. Pet. Eng. J. (March, 1965) 37,44.

/2/ Gondouin, M., Iffly, R. and Husson, J.: "An Attempt to Predict the Time Dependence of Well Deliverability in Gas Condensate Fields, "Soc. Pet. Eng. J. (June, 1967) pp. 113-124.

/3/ Ham, J.D., Brill, J.P. and Eilerts, C.K.: "Parameters for Computing Pressure Gradients and the Equilibrium Saturation of Gas-Condensate Fluids Flowing in Sandstones", Paper SPE 4037 presented at SPE 47th Annual Fall Meeting, October 1972.

/4/ Wagner, O.R. and Leach, R.O.: "Effect of Interfacial Tension on Displacement Efficiency", Society of Petroleum Engineers Journal (December 1966), pp. 335-344.

/5/ Bardon, C. and Longeron, D.G.: "Influence of Very Low Interfacial Tensions on Relative Permeability", Society of Petroleum Engineers Journal (October 1980), pp. 391-401.

/6/ Asar, H. and Handy, L.L.: "Influence of Interfacial Tensions on Gas/oil Relative Permeability in a Gas-Condensate System", SPE Reservoir Engineering (February 1988), pp. 257-264.

/7/ Haniff, M.S. and Ali, J.K.: "Relative Permeability and Low Tension Fluid Flow in Gas Condensate Systems", SPE 20917 (October 1990).

/8/ Williams, J.K. and Dawe, R.A.: "Gravity Effects in Near Critical Fluids in Porous Media", J. Coll. & Interface Sci. (August, 1988), Vol. 124, No. 2, pp. 639-646.

/9/ Danesh, A., Henderson, G.D., Krinis, D. and Peden, J.M.: "Experimental Investigation of Retrograde Condensation in Porous Media at Reservoir Conditions", SPE 18316 (October, 1988).

/10/ Saeidi, A. and Handy, L.L.: "Flow and Phase Behaviour of Gas-Condensate and Volatile Oils in Porous Media", Paper SPE 4891 presented at SPE 44th Annual California Regional Meeting, April 1974.

/11/ Ronde, H.: "Effect of Low Interfacial Tensions on Relative Permeabilities in some Gas Condensate Systems", SPE 25072 (November 1992).

/12/ Gravier, J.F., Lemouzy, P., Barroux, C. and Abed, A.F.: "Determination of Gas Condensate Relative Permeability on Whole Cores under Reservoir Conditions", Paper SPE 11493, presented at the SPE Middle East Oil Manama, Bahrain, Technical Conference, March 14-17, 1983, 7 p.

/13/ Eldon, M. and Puckett, D.: "Critical and Trapped Hydrocarbon Saturations in a Condensate Reservoir", Paper SPE 20918, presented at Europec 90, The Hague, 22-24 October, 1990.

/14/ Morel, D.C., Lomer, J.F., Morineau, Y.M. and Putz, A.G.: "Mobility of Hydrocarbon Liquids in Gas Condensate Reservoirs: Interpretation of Depletion Laboratory Experiments", SPE 24934, October 1992, presented at the 67th Annual Conference and Exhibition of SPE, Washington DC, October 4-7, 1992.

/15/ Corey, A.T.: "The Interrelation Between Gas and Oil Relative Permeabilities". Producers Monthly, November 1954, pp. 38 - 41.